

# Stabilized, Integrated, Far-Infrared Laser System for NASA/Goddard Space Flight Center

Eric R. Mueller, Joel Fontanella, and  
Robert Henschke  
DeMaria ElectroOptics Systems, Inc.  
1280 Blue Hills Ave.  
Bloomfield, CT 06002  
(806) 243-9557

## Abstract

DeMaria ElectroOptics Systems (DEOS) has delivered a highly-integrated, turn-key, Far-Infrared laser system to NASA/Goddard Space Flight Center, as a precursor for a system for SOFIA. This system has a number of unique features including: a permanently sealed-off 100W-class pump laser, an absolute heterodyne frequency lock for the pump laser, a folded extended-service sealed-off FIR laser, all electro-optics integrated within a compact easily transported housing, and a GUI controller. The absolute frequency lock not only simplifies the automated tune-up algorithms, but also improves the day-to-day absolute frequency reproducibility of the FIR output. This laser system is designed to be an instrument that can be successfully operated without extensive knowledge on the part of the user. The specifications, design, and performance results will be presented here.

This work was supported by NASA/Goddard Space Flight Center under contract number NAS5-97007.

## Introduction

The Stabilized Integrated Far-Infrared laser system (SIFIR, pronounced sī-fire) for NASA/Goddard represents a significant advancement in the state-of-the-art for FIR laser systems.

The initial design goals for the system were concentrated on ease of use, portability, and frequency & amplitude stability, and are presented in Table 1. As will be described later, the majority of these goals were met either by direct demonstration or by design analysis.

Table 1: SIFIR initial design goals.

Characteristic	Priority	Goal
Reliability	1	Operate without service for > 5000 hours
Amplitude Stability	1	<5 % long term <1 % short term
Ease Of Use	1	Autonomous starting and lockup, GUI interface displays multiple statuses, sealed-off FIR operation (see next characteristic)
FIR Operate Sealed-Off	1	Operate for 12 hrs with <10% degradation in output power
Range of Operation	1	1-3 THz
Prime Power	1	208-240 VAC, <3500 W
Long-Term Absolute Frequency Stability	2	300 kHz @ 2 THz over 8 hours after thermalization
Integrated Linewidth	2	< 50 kHz @ 2 THz
Package Size	2	<12x12x40" – head Rack mount – controller
Durability	2	Handling consistent with periodic transport
Parameter Recording	3	Software write file of system parameters vs time
Mass	3	50 kg for the laser head
Internal FIR Power Monitor	3	An internal FIR power detector

The SIFIR system uses the same permanently-sealed-off CO<sub>2</sub> laser technology DEOS employs in its commercial CO<sub>2</sub> lasers and in the space-based FIR system presently under construction at DEOS.<sup>1</sup> The FIR laser

technology used in the SIFIR is a combination of: development for the space-based FIR system, previous development for radar applications, and design efforts focussed on this program's needs.

### SIFIR Configuration

The configuration for the SIFIR system is illustrated in the photographs presented in Figure 1 and Figure 2, the drawing shown in Figure 3, and in the block diagram displayed in Figure 4. The form of the controller module was dictated by Goddard's requirements. The controller could just as easily be a 24x24x22" box and a separate lap-top computer for the GUI interface.

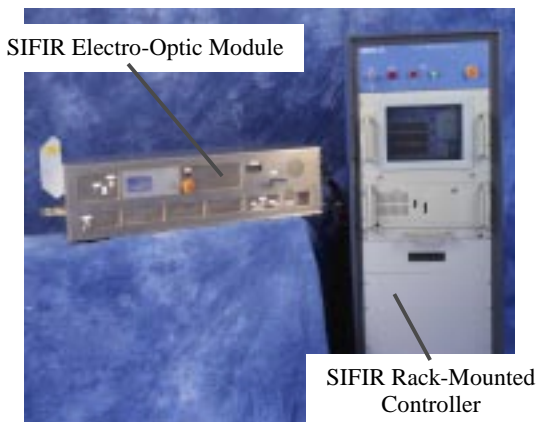


Figure 1: Photograph of the SIFIR system with the rack-mounted controller.

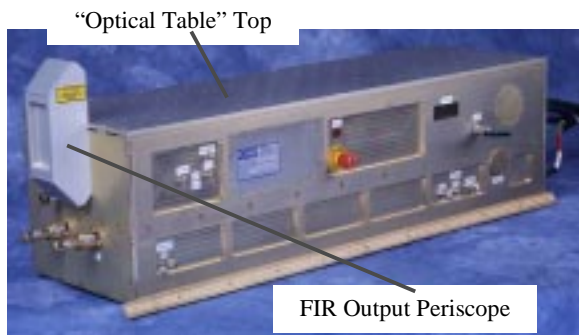


Figure 2: Photograph of the SIFIR Electro-Optic Module (laser head).

The control module contains: the laser RF power supplies, the main power

interface, the system DC power supplies, and the GUI control computer.

The Electro-Optic Module (EOM) contains: the pump laser, the local oscillator (LO) laser, the FIR laser, the IF offset-lock electronics, the LO hill-climber loop electronics, and the local loop supervisory micro processor ( $\mu\text{P}$ ).

The EOM is arranged in a "two-deck" H-structure where the pump laser and LO laser are located on the "bottom deck" and the FIR laser is located on the "top deck". The FIR gas handling system is integrated within the housing and offers access to four gas sources via "flip" valves located on one end of the EOM housing.

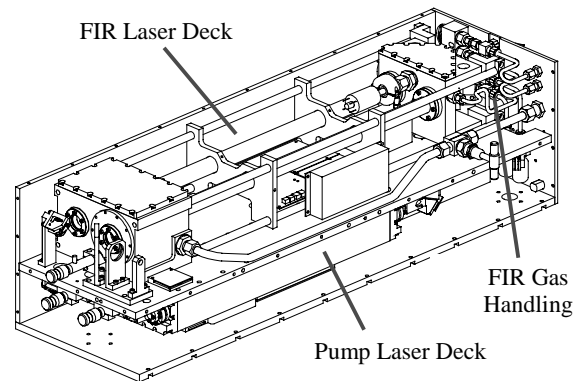


Figure 3: Drawing of the SIFIR EOM with the sides removed.

Both of the  $\text{CO}_2$  lasers are RF-excited and permanently sealed-off; the FIR laser operates sealed-off with an output degradation of less than 10 % in 12 hours, and can be operated without re-pumping for days at a time. The limitations on sealed-off operation of the FIR laser are caused by the use of elastomeric o-rings in several locations. These o-rings were used to provide for easy change of output couplers.

While the system runs reliably it has some behavior which will be improved prior to use on SOFIA. This behavior manifests itself as a requirement for the user to make slight adjustments to the pump laser differential micrometer grating control after

the first 20 minutes of operation and then potentially every 4-5 hours if the environmental temperature changes by  $\sim 5$  C over that time. There are primarily two causes for this undesired behavior. First, with the objective of obtaining larger pump powers at the weaker pump lines a non-standard waveguide geometry was selected. While this did have the effect of increasing the output power it did so at the expense of a significant increase in alignment sensitivity. Before the system was delivered, the alignment was eventually optimized for sensitivity instead of output power, effectively removing a large percentage of the output power gains achieved with the non-standard guide geometry. The second issue relates to the pump laser mounting option. In order to minimize package size, the pump laser was mounted directly to the housing center plate. While this mounting arrangement was also used for the LO laser and functioned very well in that case, in the pump laser it increased the alignment sensitivity of the pump laser, owing to the pump laser's lower stiffness ratio. This was further exacerbated by the waveguide geometry issue. In the future the pump laser will be mounted via a 3-point mount to the EOM housing. This will slightly increase the package height but Goddard has indicated that this will be acceptable.

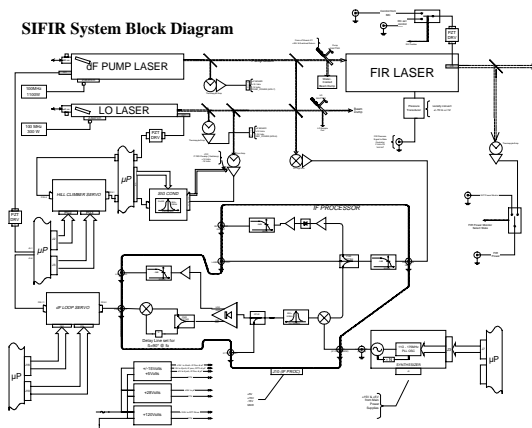


Figure 4: Block diagram of the SIFIR system.

The block diagram presented in Figure 4 illustrates the system interconnectivity and shows where functions are controlled by the  $\mu$ P vs by the system GUI controller. This block diagram will be further explained in the next section where the details of the pump frequency locking method are presented.

### Pump Laser Frequency Control

The pump frequency control approach is illustrated in Figure 5. In operation the pump and LO laser's gratings are set to the same rotational line. The LO laser is dither-stabilized to its line-center to form a frequency reference at the  $\text{CO}_2$  frequency. A small sample of the pump laser is then mixed with this LO laser in a

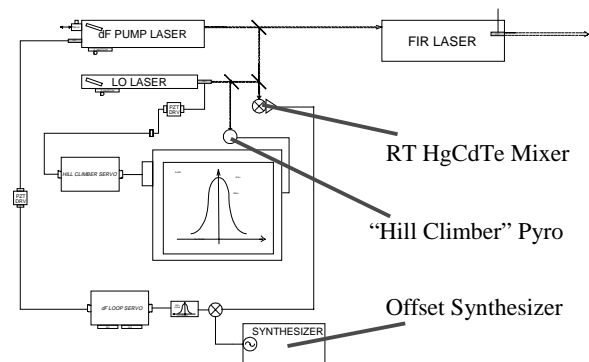


Figure 5: Block diagram of the pump-frequency locking technique.

room temperature HgCdTe mixer. This IF is then mixed with an offset synthesizer. The resulting IF is processed through a delay discriminator to generate an error signal for the pump laser piezoelectric transducer (PZT) control. The sign of the offset (ie. below or above  $\text{CO}_2$  line center) is set with a simple sign flip in the error loop circuitry.

The minimum offset obtainable with this topology is determined by the narrowness and steepness of the last IF filter in the discriminator. In the present system a surface-acoustic-wave filter was employed and the minimum offset magnitude settable

for stable performance was 3 MHz. This minimum offset is sufficient to pump almost any FIR line optimally and any FIR line slightly off optimal.

The approach used in this work for absolute pump frequency control is very similar to an earlier technique applied for investigation of Autler-Townes splitting<sup>2</sup> and is a marked improvement in utility over the 4.3  $\mu\text{m}$  fluorescence Lamb dip locked LO used in the past<sup>3</sup> (as that technique requires a cooled detector and a cumbersome setup). However the fluorescence technique offers better absolute pump frequency accuracy (on the order of 3 kHz vs on the order of 100 kHz for the present technique) but this additional accuracy is not relevant for most FIR pumping applications.

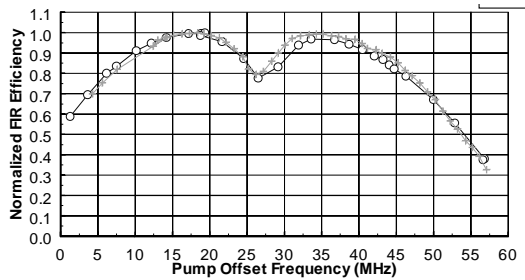


Figure 6: FIR laser efficiency vs pump frequency for a standing-wave resonator operating the 118.83  $\mu\text{m}$  line in  $\text{CH}_3\text{OH}$ .

In considering the implications of absolute pump frequency control one can look at the FIR efficiency vs pump frequency curve for a standing-wave FIR laser operating on the 118.83  $\mu\text{m}$  line in  $\text{CH}_3\text{OH}$  (see Figure 6). The behavior observed there is due to bi-directional pumping creating a “transferred” Lamb dip in the FIR gain.<sup>4</sup> Thus to tune-up such a FIR laser system the user must find both the optimal pump frequency and the optimal FIR cavity length. Owing to the broadness of the efficiency curve this process will tend to have a reproducibility error on the order of 5-10 MHz, depending on line. This error

will then be transferred to the FIR via Doppler pulling and absorption frequency pulling, and manifest itself as a FIR frequency reproducibility error. A lower limit estimate of this error can be calculated from the Doppler-only portion with

$$\Delta\nu = \nu_{epump} \left[ \frac{\nu_{FIR}}{\nu_{pump}} \right], \quad (1)$$

where  $\Delta\nu$  is the FIR frequency error,  $\nu_{epump}$  is the pump frequency error,  $\nu_{FIR}$  is the nominal FIR frequency, and  $\nu_{pump}$  is the nominal pump frequency. This effect is enhanced by absorption frequency pulling and was recognized in the past and its effect measured.<sup>5</sup> Depending on the FIR line this error can be on the order of 0.1 – 1 MHz. In many applications this magnitude of error is not significant but in sub-Doppler spectroscopy this effect can be quite significant.

While this certainly does not exhaust the sources of frequency error it is a significant contributor even in a stabilized FIR system. Another contributor, the pressure dependence of FIR frequency, is mitigated in this system by the fact that the FIR laser operates sealed-off – improving both the knowledge of pressure in the cell and the control & stability of that pressure.

The pump frequency control approach used here is one of the major features of this system. With this configuration the pump laser’s offset can be directly set via the offset-synthesizer. This offers dramatic advantages not only in FIR frequency reproducibility, but also in easy tune-up.

The tune-up advantages stem from the fact that the pump laser’s frequency can be directly set to the optimal point. Thus there is no need to separately optimize this control at start-up. The user simply sets the offset for optimal and then adjusts the FIR cavity length for optimal output.

Additionally the SIFIR system becomes a tool for determining the absolute optimal offset for any FIR line. In the SIFIR system the  $\mu\text{P}$  handles the locking and monitoring of the LO and pump loops, providing for a simple GUI to allow the user to select the pump frequency.

It should also be noted that the pump laser is a true waveguide laser and has NO mode adjustments required or available to the user.

### Integration Optics

The optical system which integrates this system consists of several parts: the pump – to – FIR laser optics, the heterodyne-offset optics, and the FIR power sampling optics.

A photograph of the pump deck of the SIFIR is presented in Figure 7. In that

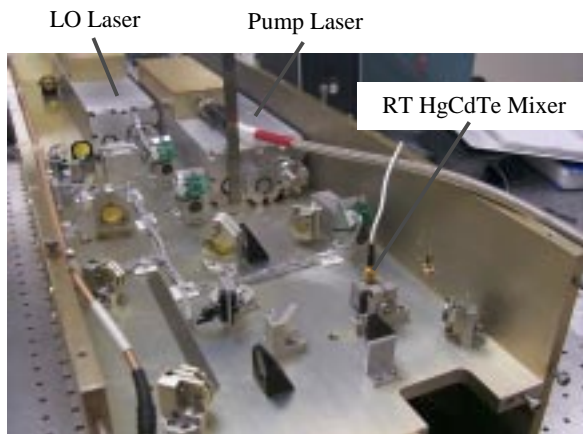


Figure 7: Photograph of the pump deck of the SIFIR EOM. Note 6" rulers for scale.

figure both  $\text{CO}_2$  lasers and all of the  $\text{CO}_2$  optics (except for the two mirrors which direct the pump beam into the FIR laser) are visible.

A plan view of the heterodyne optical area of the pump deck is shown in Figure 8. The solid red line represents the pump beam path, and the dashed blue line represents the LO beam path. Also visible are two shutters and two beam dumps.

These serve to: allow the user to operate the system without exciting the FIR laser, via the pump beam shutter and its water-cooled beam dump, and to send the majority of the LO beam out of the EOM to check the grating calibration or allow it to be “dumped” into the chill-plate-mounted LO beam dump. Both of these shutters are controlled and monitored via the GUI and  $\mu\text{P}$ .

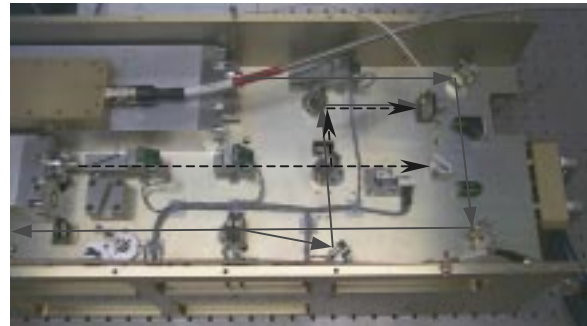


Figure 8: Plan view photograph of the heterodyne-offset optics area of the SIFIR. The solid (red) line represents the pump beam path. The dashed (blue) line represents the LO beam path.

The FIR power sampling optics consist of a  $8\ \mu\text{m}$  Mylar beamsplitter, a 50 mm focal length polyethylene lens, and a FIR thermopile detector. While this technique has significant wavelength and polarization dependence, the GUI software provides for independent individual calibration for each FIR line or use of an external power monitor also read by the SIFIR’s controller.

### FIR Laser

The FIR laser is a thermally-compensated design where the cavity length is set via a differential micrometer and/or PZT, and this length is maintained through thermal compensation. DEOS staff have extensive experience with this design approach and have obtained frequency stability results of 35 kHz over many hours after thermalization. Additionally, through

careful attention to thermalization alignment issues, this laser needs NO alignment adjustments; only the cavity length ever needs user adjustment.

The finite element analysis (FEA) results used in the thermal compensation design of the FIR laser are presented in Figure 9. Those results are only valid after warm-up and indicate a compensation frequency performance of 26 kHz/C at 200  $\mu\text{m}$ . From cold-start to thermalization the uncompensated FIR cavity length change was found to be

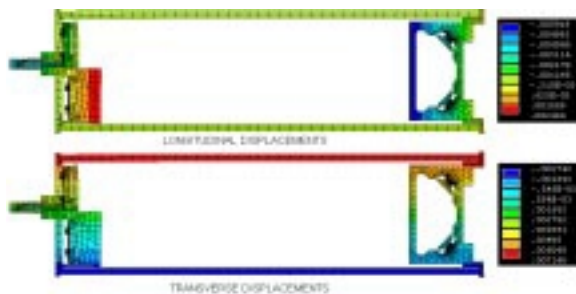


Figure 9: FEA results for the thermal compensation of the FIR laser. (These results are only valid after thermalization.)

15 - 18  $\mu\text{m}$ . This is a convenient result as the FIR PZT has a range of 20  $\mu\text{m}$  and the GUI program includes an FIR auto-tuning algorithm which can periodically correct for this change during warm-up. The 3  $\mu\text{m}$  range of this measurement is due primarily to submicron-scale slip-stick thermalization shifts from one day to the next.

A photograph of the FIR laser is presented in Figure 10. The FIR laser is a folded standing-wave cavity with quartz

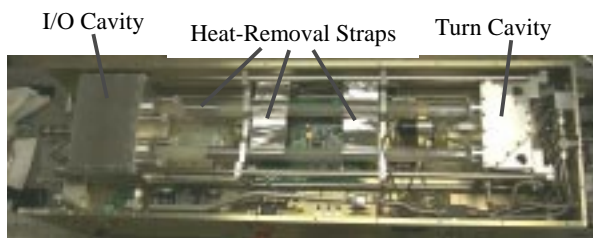


Figure 10: Photograph of the FIR laser.

waveguide sections and ferro-fluid alignment feedthroughs. Heat is removed from the guide sections via metal straps secured from the guides to the water-cooled housing. This basic laser design could also be embodied in a ring configuration by changing the I/O cavity. FIR pressure is measured with a Pirani gauge. While this gauge has a gas composition dependence, it is perfectly applicable as a reference-for-optimal gauge.

The FIR laser performed well in spatial mode, stability, and output power. While the folded design decreases the size of the laser it also decreases its efficiency by roughly a factor of 1.7. At 118.83  $\mu\text{m}$  in  $\text{CH}_3\text{OH}$  we obtained 125 mW in a clean spatial mode (see Figure 11). The stability

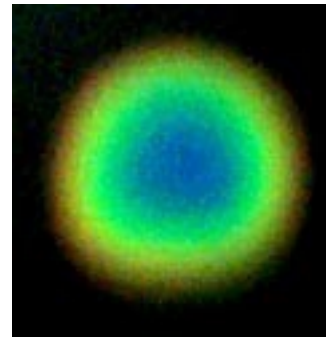


Figure 11: Spatial mode of the FIR laser at 118.83 $\mu\text{m}$ . (This is a digital picture of a liquid crystal sheet image.)

of the output is viewed in two different timescales: hours, and minutes. The long-term (over hours) stability was 5 %. This was dominated by thermal effects in the FIR-to-pump laser feedback. The short-term stability (over minutes) was <0.2 %.

In typical operation the user simply pumps the FIR laser out, fills the laser to the desired pressure, closes off the pump, and shuts the pump down. The user can then expect the system to operate satisfactorily all day (or even longer) without any additional service.

## Graphical User Interface (GUI) Controller

The GUI controller is another major feature of this SIFIR system. It provides for the easy operation and monitoring of the system by a user with little specific laser knowledge. The system can be operated in a “manual” start-up mode or in an auto start-up mode.

In manual mode (or after auto start-up completes) the CO<sub>2</sub> lasers and their frequency locks are controlled with virtual buttons on the screen. Also displayed on the screen are other system parameters including: the status of all of the lasers, their respective PZT voltages, the FIR pressure, and the FIR power. The user has the option of changing FIR lines (either choosing from the catalog or manually optimizing a “new” line) or writing parameters for a “new” line into the catalog.

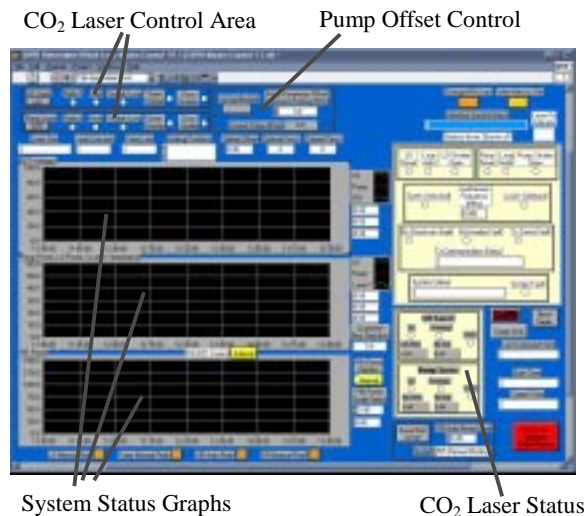


Figure 12: Screen “shot” of the GUI controller user interface.

In auto start-up, the user selects the desired line from the catalog and the system locks the lasers and prompts the user when FIR pumping can begin. At this point the user checks the pressure in the FIR laser against the optimal pressure recorded in the on-line catalog and presses the “Open Pump Shutter” button to begin exciting the FIR

laser. In any mode the user has the option of having the system write a telemetry file which records user and system actions/status every ~3 seconds.

The automatic locking of the pump laser is at the heart of the autonomous operation of the SIFIR. A temporal view of the auto pump lock algorithm is presented in Figure 13. The algorithm ramps the pump PZT and looks at the IF log video to determine if the pump laser is near the correct frequency offset magnitude, and then looks at the order in which the Freq Hi and Freq Lo bits toggle to determine if the sign is correct. Once the correct offset has been found the  $\mu$ P sets the pump PZT to this position and closes the pump frequency control loop via a MDAC. When the system is first turned on (for the first 15-20 minutes) this algorithm will not work reliably as the cavity length is drifting too rapidly for the PZT reset portion to leave the pump laser at the correct frequency for lock capture.

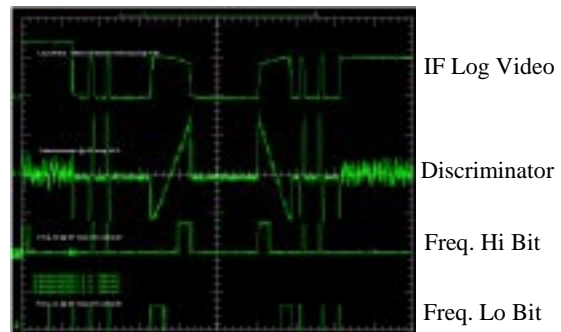


Figure 13: Temporal view of the autonomous acquisition algorithm for the pump-laser offset frequency.

To automatically determine if the LO loop or the pump loop need resetting, the  $\mu$ P monitors the PZT voltages and initiates a reset if these PZT voltages get within 10 % of max or min voltage.

## System Performance

The system performance can be compared against the goals laid out in Table

1. This comparison is presented in Table 2. All the goals but one were met. The laser head mass goal (which was lower priority) was 50 kg and in the delivered system the head mass was 54 kg. The issue of occasional pump grating differential micrometer adjustments while not desirable, did not significantly degrade the usability of the system. Effectively this system is operated with occasional (every 4-5 hours) user adjustment of two controls: the FIR cavity length, and the differential control on the pump laser grating mount. In the future this

Table 2: System performance against initial goals.

Characteristic	Met	Measured How
Reliability	Yes	Life data from similar pump and FIR lasers
Amplitude Stability	Yes	Tested <5 % over many hours <0.2 % over minutes
Ease Of Use	Yes	GUI-driven control of all major functions
FIR Operate Sealed-Off	Yes	Tested
Range of Operation	Yes	Tested from 1.2 – 3.1 THz
Prime Power	Yes	208-240 VAC, 3000 W
Long-Term Absolute Frequency Stability	Yes	Analysis & pump locking reproducibility measurements (Lamb dip)
Integrated Linewidth	Yes	Measurements of pump width and comparison of measurements with similar systems
Package Size	Yes	Measured 12x12x38"
Durability	Yes	Measured performance before and after repeated moves.
Parameter Recording	Yes	Software write file of system parameters vs time
Mass	No	Goal was 50 kg, actual is 54 kg
Internal FIR Power Monitor	Yes	Internal detector present and used by controller.

system will operate with only one user adjustment, the FIR cavity length control. And even that control does not require adjustment after thermalization.

## Conclusions

The SIFIR system delivered to Goddard Space Flight Center is a FIR laser appliance. While the user has access-to and control-of the system parameters in great detail, these parameters are normally set and maintained by the autonomous computer controller. This approach yields a “user system,” where the user can concentrate on the measurement at hand instead of making the laser work.

## Acknowledgements

The authors would like to acknowledge the contributions to this project of a number of talented scientists and technologists including: Adrian Papanide, Shef Robotham, Gordon Chin, Lanny Laughman, Leon Newman, John Kennedy, and Dick Hart.

## References & End Notes

- <sup>1</sup> E. R. Mueller, W. E. Robotham, Jr., R. P. Meisner, R. A. Hart, J. Kennedy, and L. A. Newman, “2.5 THz Laser Local Oscillator for the EOS CHEM 1 Satellite,” Proc. Ninth Int. Symp. Space THz Techno., 563 (1998)
- <sup>2</sup> C. R. Pidgeon, W. J. Firth, R. A. Wood, A. Vass, and B. W. Davis, “Two-Photon Light Shift and Autler-Townes Splitting in Optically-Pumped FIR Lasers,” Int. J. IR MMW, **2**(2), 207 (1981)
- <sup>3</sup> B. Dahmani & A. Claron, “Frequency Stability Limitations of Optically Pumped Lasers Due to Pump Laser Instability Through Dispersion Effect,” Int. J. IR MMW, **5**(7), 1053 (1984)
- <sup>4</sup> The situation is different in ring FIR lasers which switch direction near the FIR absorption center. But this technique would be applicable and potentially even more important for ring laser pumping.
- <sup>5</sup> R. L. Crownover, H. O. Everitt, F. C. DeLucia, and D. D. Skatrud, “Frequency stability and reproducibility of optically pumped far-infrared lasers,” Appl. Phys. Lett, **57**(27), 2882 (1990)